Quantitative Characterization of Three Carbonic Anhydrase Inhibitors by LESA Mass Spectrometry

Illes-Toth, Eva; Stubbs, Christopher J; Sisley, Emma K; Bellamy-Carter, Jeddidiah; Simmonds, Anna L; Mize, Todd H; Styles, Iain B; Goodwin, Richard J A; Cooper, Helen J

DOI:
10.1021/jasms.2c00024

ACS Partner Journal

Journal of the American Society for Mass Spectrometry

pubs.acs.org/jasms

Research Article

Quantitative Characterization of Three Carbonic Anhydrase Inhibitors by LESA Mass Spectrometry

Eva Illes-Toth, Christopher J. Stubbs, Emma K. Sisley, Jeddidiah Bellamy-Carter, Anna L. Simmonds, Todd H. Mize, Iain B. Styles, Richard J. A. Goodwin, and Helen J. Cooper*

Cite This: *J. Am. Soc. Mass Spectrom.* 2022, 33, 1168−1175

Read Online

ACCESS | Metrics & More | Article Recommendations | Supporting Information

ABSTRACT: Liquid extraction surface analysis (LESA) coupled to native mass spectrometry (MS) presents unique analytical opportunities due to its sensitivity, speed, and automation. Here, we examine whether this tool can be used to quantitatively probe protein−ligand interactions through calculation of equilibrium dissociation constants (K_d values). We performed native LESA MS analyses for a well-characterized system comprising bovine carbonic anhydrase II and the ligands chlorothiazide, dansylamide, and sulfanilamide, and compared the results with those obtained from direct infusion mass spectrometry and surface plasmon resonance measurements. Two LESA approaches were considered: In one approach, the protein and ligand were premixed in solution before being deposited and dried onto a solid substrate for LESA sampling, and in the second, the protein alone was dried onto the substrate and the ligand was included in the LESA sampling solvent. Good agreement was found between the K_d values derived from direct infusion MS and LESA MS when the protein and ligand were premixed; however, K_d values determined from LESA MS measurements where the ligand was in the sampling solvent were inconsistent. Our results suggest that LESA MS is a suitable tool for quantitative analysis of protein−ligand interactions when the dried sample comprises both protein and ligand.

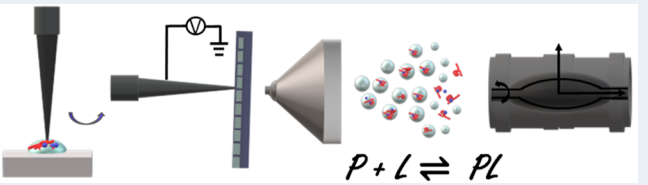

INTRODUCTION

Protein−ligand binding is of key importance in all living organisms for the maintenance of protein structure and function, enzymatic activity, molecular interactions, signaling, and recognition. Therapeutic interventions exploit noncovalent interactions between the drug ligand and the target protein. Understanding the binding characteristics, e.g., stoichiometry, equilibrium dissociation constants, binding sites, and nature of binding (covalent vs noncovalent interactions), is therefore of paramount importance in the discovery and development of drugs. Detailed characterization of these essential parameters can be performed by an array of analytical techniques including mass spectrometry (MS),[1] isothermal titration calorimetry (ITC),[2] surface plasmon resonance (SPR),[3] fluorescence spectroscopy, fluorescence correlation spectroscopy (FCS),[4] and nuclear magnetic resonance (NMR).[5,6]

Native MS in conjunction with nanoelectrospray ionization (nESI), herein referred to as direct infusion for simplicity, has been widely exploited for the quantitative analysis of protein−ligand and protein−protein interactions,[7] including for the characterization of protein−small molecule,[8−10] protein−phosphopeptide,[11] protein−carbohydrate,[12,13] protein−protein,[14] protein−DNA,[15] and protein−RNA[16] complexes. Broadly, the capabilities of direct infusion MS for the study of protein−ligand binding are twofold. First, the resultant mass shift, as detected in the mass spectrum, is indicative of binding of a ligand to a protein. Second, the relative intensities of unbound protein ion peaks and ligand-bound protein ion peaks can be used to quantitatively monitor the extent of binding. Typically, the concentration of the protein of interest is fixed, and the ligand concentration is varied in order to perform a titration. With increasing ligand concentrations, a proportional increase in the intensity of the ligand-bound peak is observed.[17] The ratio of the protein−ligand complex and the protein, referred to as the response (R), is plotted as a function of initial ligand concentration.[15,18−20] This plot serves as the basis for determination of the equilibrium dissociation constant (K_d) via curve fitting with a linear[19] or nonlinear function.[12] The relative intensities or peak areas of the ligand-free and ligand-bound peaks are expressed for all observed charge states rather than for individual charge states in order to obtain a more comprehensive picture: individual charge states may disproportionally represent single, distinct conformational forms.[9,21]

Protein−ligand titrations monitored in the gas phase assume that the ionization efficiency of unbound protein and the protein−ligand complex is similar in the case of a small ligand

Received: January 21, 2022
Revised: May 12, 2022
Accepted: May 16, 2022
Published: June 8, 2022

that does not substantially increase the mass and that the initial protein concentration does not change during the ionization and detection process.[17,22] Nevertheless, source conditions and instrumental parameters can affect the stability of complexes, necessitating cautious interpretation of the derived equilibrium dissociation constants.[11,12,14,19,23] Minimization of in-source dissociation of low-affinity, labile complexes is a critical step of gas-phase titrations and can be experimentally achieved through optimal selection of tuning conditions, reducing the diameter of the electrospray emitter, and/or application of a postacquisition correction to account for partial in-source dissociation.[24,25] The use of complementary in-solution techniques has proven to be helpful for further validation.[26,27]

Here, we sought to evaluate the use of liquid extraction surface analysis (LESA)[28] MS for the measurement of binding affinities under native-like conditions. Native LESA MS appears to be an attractive strategy for the study of protein−ligand or protein−protein interactions as it affords automation prior to MS, allows direct sampling from a solid surface, and has the potential to lend itself to measurement of binding affinities in *ex vivo* tissue samples. Indeed, we have demonstrated analyses of endogenous protein assemblies and protein ligands from thin tissue sections by native LESA MS.[29−31] As an initial step in exploring the utility of LESA for quantitative analysis of protein−ligand binding, we examine the utility of native LESA MS for the measurement of K_d values by use of a well-characterized model system comprising bovine carbonic anhydrase (CAH) and three ligands, chlorothiazide (CTZ), dansylamide (DNSA), and sulfanilamide (SLFA) (Figure S1, Supporting Information). In numerous previous biophysical studies, CTZ,[9,32] DNSA,[32,33] and SLFA[27,34,35] have shown to be potent inhibitors of various isoforms and derivatives of CAH. The carbonic anhydrases are a large group of isoenzymes,[34,36] some of which are membrane bound while others are cytosolic or secreted, that catalyze the interconversion of CO_2 and bicarbonate.[37] They represent key pharmaceutical targets owing to their involvement in infection, cancer, glaucoma, obesity, and hypertension.[36,38] Bovine CAH is a particularly well-described model protein, a 259-residue enzyme[39] that catalyzes the hydration of carbon dioxide and dehydration of bicarbonate.[37] In its hydrophobic, active center it contains a Zn^{2+} ion coordinated by three imidazole moieties and a hydroxide group to which many of its inhibitors bind.[40−42] Sulfonamides and their derivatives, e.g., SLFA and CTZ, bind to CAH via coordination to the Zn^{2+} in the center of the binding pocket.[36,40,43] The aromatic rings of Zn^{2+} binders can occupy both the hydrophobic and the hydrophilic parts of the binding cavity, whereas the tails tend to orient toward the exit of the binding pocket.[36] DNSA favors the hydrophobic region of the binding pocket with its naphthalene ring rotated in a 54° angle.[44]

We compared K_d values measured by direct infusion MS with those measured by LESA MS. Two LESA strategies were trialled. In the first, the protein and ligand were mixed in solution prior to deposition and drying on a foil-covered glass slide. The resulting dried protein/ligand spots were sampled by LESA using a solvent comprising 25 mM ammonium acetate. We refer to this approach as "$LESA_{premix}$". In the second, solutions of the pure protein were deposited and dried onto foil-covered glass slides. The dried protein spot was sampled with a solvent comprising 25 mM ammonium acetate which contained the ligand. We refer to this approach as "$LESA_{ligand}$". To corroborate our data, K_d values determined by MS were validated against SPR measurements. SPR is a label-free, surface-based, optical technique commonly deployed for the characterization of macromolecular interactions.[45,46]

EXPERIMENTAL SECTION

Sample Preparation. Ten micromolar bovine carbonic anhydrase II (CAH) was mixed with various concentrations of CTZ, DNSA, and SLFA in 25 mM ammonium acetate (pH 7.0), incubated for 10 min at room temperature (21−22 °C), and processed by direct infusion nESI MS or by native LESA MS. LESA was performed by use of the Triversa Nanomate platform (Advion, Ithaca, NY). Full details of the sampling procedures are described in the Supporting Information and summarized below.

$LESA_{premix}$. A 1.5 μL amount of 10 μM CAH only or [CAH + ligand] was spotted onto a microscope glass slide covered with a layer of Al foil and allowed to air dry at room temperature. The dried spots were sampled with 25 mM ammonium acetate (pH 7.0) with a dwell time of 60 s following aspiration of 5.0 μL of solvent and deposition of 3.0 μL. A 3.5 μL amount was reaspirated to ensure complete sample collection.

$LESA_{ligand}$. A 1.5 μL amount of 10 μM CAH was spotted onto a microscope glass slide covered with Al foil and allowed to air dry at room temperature. The dried spots were sampled with 25 mM ammonium acetate (pH 7.0) containing various concentrations of CTZ, DNSA, or SLFA at room temperature. The sampling protocol was comprised of 10 mix and repeat cycles at the settings above to control for the 10 min incubation used for $LESA_{premix}$.

Mass Spectrometry and Data Analyses. All protein−ligand titration experiments were performed on an Orbitrap Elite mass spectrometer (Thermo Fisher Scientific, Bremen, Germany) with an automatic gain control target of 1×10^6 charges in full-scan mode, 250 °C source temperature, 25−30% RF voltage, 5 or 10 ms injection time, 1000 microscans, and 120 000 resolution. Data were acquired in triplicate in the 200−4000 m/z mass range for 3−5 min. The ion intensities of each acquisition were summed in Xcalibur (Foundation 3.0 SP2), written to a raw file, and further processed in MATLAB (version R2017a and statistics toolbox, Mathworks, Inc., Natick, MA) and Python (version 3.7.6) using in-house software (see Supplemental File 1, Supporting Information). Using MATLAB, the peak areas of protonated unbound and ligand-bound protein peaks in all observed charge states (9+, 10+, and 11+) were determined using the trapezium rule. The average ratio, R, of bound to unbound protein across the three charge states was determined. No baseline correction was performed, and only the main protonated ion was considered. Titration curves were then generated in Python. The mean fraction bound ($R/(R + 1)$) from experimental replicates was plotted as a function of the initial ligand concentration L_0 (μM).

Equilibrium dissociation constants were then calculated by fitting the titration curves using a nonlinear sum of least squares. In the case of direct infusion measurements, equilibrium dissociation constants were calculated by fitting the titration curves to eq 1 (described in detail in ref 25), where P_0 denotes the initial protein concentration, K_d is the equilibrium dissociation constant, and f_{sat} is a correction factor to account for gas-phase dissociation and is the experimental bound fraction at saturation.

https://doi.org/10.1021/jasms.2c00024
J. Am. Soc. Mass Spectrom. 2022, 33, 1168−1175

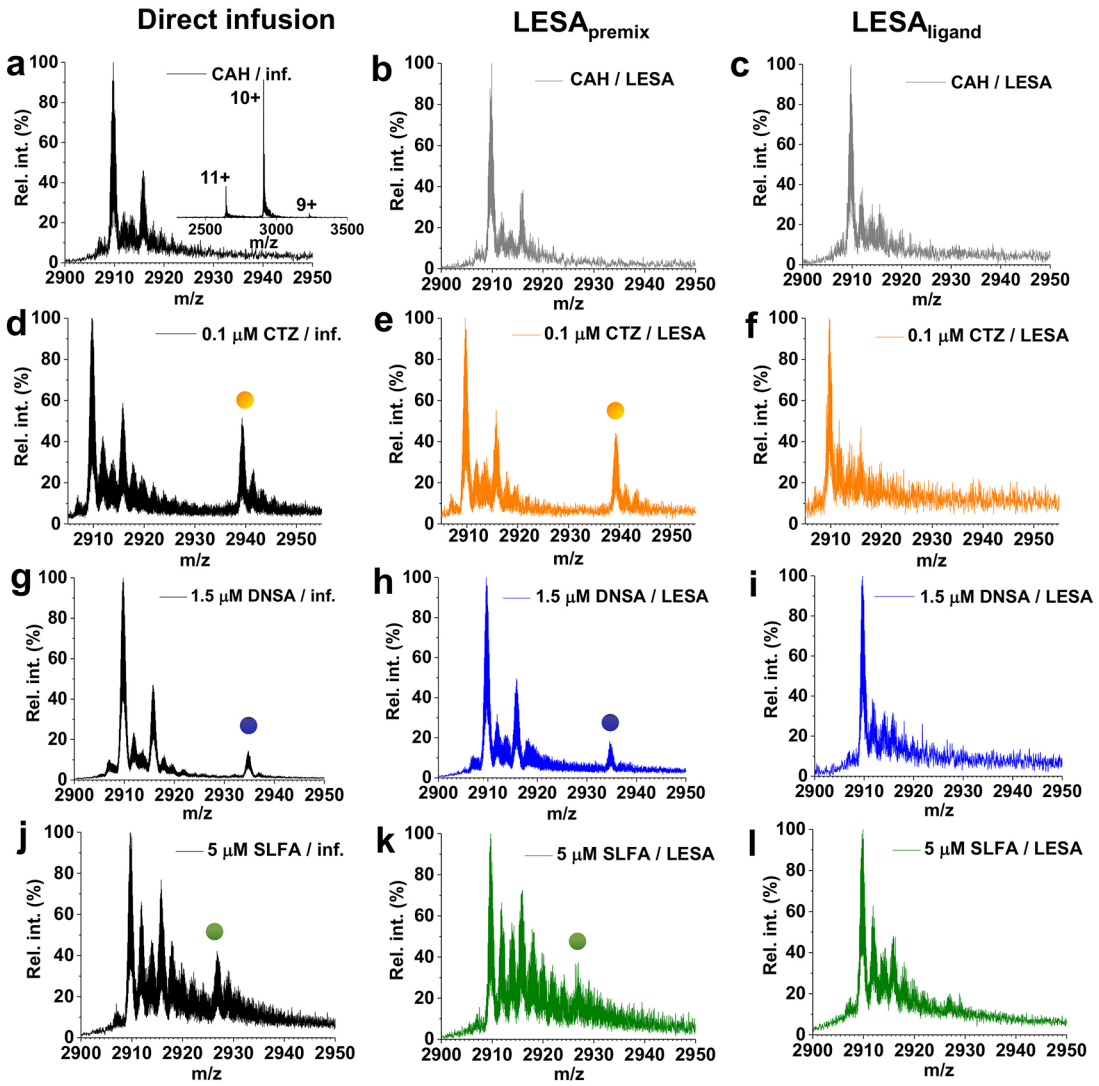

Figure 1. Native mass spectra of CAH following direct infusion (a), $LESA_{premix}$ (b), and $LESA_{ligand}$ (c) sampling. (Inset) CSD of CAH in its Zn^{2+}-bound form with the 10^+ ion being the most abundant. Native mass spectra of CAH in the presence of 0.1 μM CTZ following direct infusion (d), $LESA_{premix}$ (e), and $LESA_{ligand}$ (f). Mass spectra of CAH in the presence of 1.5 μM DNSA obtained in direct infusion mode (g) and subsequently $LESA_{premix}$ (h) and $LESA_{ligand}$ (i) sampling. Native mass spectra of CAH in the presence of 5 μM SLFA following direct infusion (j), $LESA_{premix}$ (k), and $LESA_{ligand}$ (l) sampling. Dots represent the protein−ligand complexes.

$$\frac{R}{R+1} = f_{sat} \times \frac{P_0 + L_0 + K_d - \sqrt{(P_0 + L_0 + K_d)^2 - 4P_0L_0}}{2P_0} \quad (1)$$

For the $LESA_{premix}$ and $LESA_{ligand}$ measurements, corrected values of L_0 and/or P_0 were used to account for extraction efficiency and dilution effects associated with the sampling process as described below.

Determination of P_0 Correction for Combined Protein Extraction Efficiency and Dilution Effects. *$LESA_{premix}$.* A paper grid print of a 1584-well plate was placed into the plate holder of the stage directly under the glass slide covered with Al foil containing the samples in order to guide manual selection of *xy* coordinates. In addition, a halved 96-well plate was placed beside the glass slide for collection of extracted aliquots. The advanced user interface (AUI) was used to aspirate 5 μL of 25 mM ammonium acetate and dispense that onto a 1.5 μL dried droplet of 10 μM CAH at a 3 μL/min flow rate, 1.4−1.6 mm height, mimicking the formation of a liquid junction at a 60 s dwell time. A 3.5 μL volume was reaspirated for collection into a half 96-well plate. For each location sampled (n = 15), two 1.2 μL samples were analyzed on the DeNovix DS-II spectrophotometer. The UV spectra at 280 nm (A_{280}) were used to calculate the corrected concentration (in micromolar) based on the extinction coefficient of CAH (50 070 M^{-1} cm^{-1} [47]). The absorption of 25 mM ammonium acetate was subtracted from that of CAH. Data were exported as .csv files, and the correction factor incorporating both the dilution effect and the extraction efficiency of LESA was calculated in Prism GraphPad 6.01. The mean concentration of 15 sample spots (micromolar) was used as the corrected value for P_0.

$LESA_{ligand}$. The corrected value for P_0 was determined as above except that the sampling procedure was adjusted to mimic the $LESA_{ligand}$ sampling procedure in which 10 mix and repeat steps were included. To aid sample collection, the blowout tab was checked in the software and the volume was released at a pressure of 3 psi and duration of 10 s. In total, 10 spots were sampled and analyzed as above. The mean

https://doi.org/10.1021/jasms.2c00024
J. Am. Soc. Mass Spectrom. 2022, 33, 1168−1175

Table 1. Summary of the Experimentally-Derived K_d Values, and Comparison with Literature Values*

ligand	direct infusion mean K_d ± STD (μM)	$LESA_{premix}$ mean K_d ± STD (μM)	$LESA_{ligand}$ mean K_d ± STD (μM)	SPR mean K_d ± STD (μM)	literature mean K_d ± STD (μM)
CTZ	0.28 ± 0.56	0.21 ± 0.14[a]	0.60 ± 0.52[b]	0.28 ± 0.01	2.63 ± 0.14, MS, bovine CAHII[48]
		0.26 ± 0.53[c]	0.98 ± 0.70[a]		0.06 ± 0.02, MS, bovine CAHII[9]
			0.19 ± 0.66[c]		
DNSA	12.49 ± 1.69	11.06 ± 6.75[a]	0.37 ± 0.29[b]	1.14 ± 0.32	0.34 ± 0.04, SPR, 25 °C, bovine CAHII;[33] 0.36 ± 0.04, ITC, 25 °C, bovine CAHI;[33] 0.42 ± 0.10, stopped-flow fluorescence, 25 °C, bovine CAHII[33]
		29.93 ± 23.31[c]	0.43 ± 0.31[a]		0.46 ± 0.01, fluorescence, human CAI;[49] 2.74 ± 0.08, fluorescence, human CAHII;[49] 0.84, fluorescence, bovine CAHII[49]
			0.37 ± 1.18[c]		0.45 ± 0.10, back scattering interferometry, bovine CAHII[50]
					0.44 ± 0.12, SPR, 25 °C, bovine CAHII[50,51]
SLFA	3.02 ± 1.68	1.73 ± 0.55[a]	1.66 ± 0.89[b]	4.42 ± 1.39	63.5 ± 15.8, colorim. titration, 23 °C;[35] 89.7 ± 21.7, 37 °C, human CAHI[35]
		1.89 ± 1.45[c]	1.63 ± 0.88[a]		14.9 ± 3.8, colorim. titration, 23 °C, human CAHII;[35] 28.1 ± 6.0, colorim. titration, 37 °C, human CAHII[35]
			0.22 ± 0.58[c]		0.924, SPR, 25 °C, human CAHI;[27] 145.7 ± 10, MS, human CAHI[27]
					125.5 ± 18.7, ITC, 25 °C, human CAHI[27]
					0.57 ± 0.09, back scattering interferometry, bovine CAHII[50]
					3.1 ± 1.1, SPR, 25 °C, bovine CAHII[50,51]

*Literature reference values are displayed with an indication of CAH isoform, temperature, and analytical technique if provided. K_d values determined from LESA experiments are shown before and after corrections of L_0 and/or P_0. [a]P_0 and L_0 corrected for LESA extraction efficiency and dilution. [b]P_0 corrected for extraction efficiency and dilution. [c]Uncorrected for LESA extraction efficiency and dilution.

concentration (micromolar) was used directly as the corrected value for P_0.

LESA Correction Factor for the Total Free Ligand Extraction Efficiency and Dilution Effects. The absorption spectra of different concentrations of CTZ, SLFA, and DNSA were obtained by spectrophotometry (wavelength 220−500 nm) for a solution reference curve without any sample manipulation, $n = 3$. The wavelength of maximum absorption was determined from these samples. A 1.5 μL amount of ligand was deposited on the surface of a glass slide covered with Al foil, air dried, placed on top of a 1584-well paper grid at different concentrations in order to determine its coordinates, and extracted in 25 mM ammonium acetate in triplicate using the aforementioned LESA AUI sampling conditions. The absorption spectra of the samples following LESA AUI were collected and exported as .csv files, after confirming no significant red or blue shift, in order to calculate the correction factor accounting for both dilution effects and extraction efficiency and any evaporation occurring during extended LESA sampling in the case of the $LESA_{ligand}$ for the free ligands at different concentrations. The mean and standard deviation values were calculated in Prism GraphPad 6.01 based on the solution reference values and the AUI collected samples. The mean value ± STD of the entire concentration range measured yielded the correction factor used in the K_d calculations. The mean correction factor was used to multiply the initial reference L_0 values to obtain its paired corrected L_0.

Traveling Wave Ion Mobility Spectrometry MS, Surface Plasmon Resonance, and Circular Dichroism Spectroscopy. Details are given in the Supporting Information.

RESULTS AND DISCUSSION

Figure 1 shows the mass spectra obtained following direct infusion, $LESA_{premix}$, and $LESA_{ligand}$ for CAH and the three ligands at various ligand concentrations (0, 0.1, 1.5, and 5 μM). For CAH, a typical narrow charge state distribution (CSD) was observed ranging from 9^+ to 11^+ with the 10^+ charge state being the most dominant (Figure 1a−c), indicative of retention of its native structure. The deconvoluted mass, 29 088.86 Da, revealed that CAH was N-terminally acetylated with a Zn^{2+} ion bound to the protein (Figure S2, Supporting Information) and is in good agreement (<5 ppm) with the theoretically calculated mass of the protein with 29 088.78 Da (accession ID P00921).

In the presence of CTZ, a 295 Da mass shift was observed in the direct infusion (Figure 1d) and $LESA_{premix}$ (Figure 1e) samples at concentrations of 0.1 μM and above. No obvious ligand binding was observed at 0.1 μM CTZ with $LESA_{ligand}$ MS (Figure 1f) but was observed at concentrations above 1 μM (Figure S3, Supporting Information). For DNSA, ligand binding was observed in the mass spectra (Δ 250 Da) at 1.5 μM and above in both direct infusion (Figure 1g) and $LESA_{premix}$ (Figure 1h). No ligand binding was observed following $LESA_{ligand}$ (Figure 1i) at this concentration; however, it could be observed at concentrations above 3 μM (Figure S4, Supporting Information). In the presence of SLFA, the mass spectra revealed that a 172 Da mass shift, corresponding to ligand binding, occurred from a 5 μM concentration onward in direct infusion mode (Figure 1j) and in $LESA_{premix}$ mode (Figure 1k), but a well-resolved peak for the protein−ligand complex could not be detected in $LESA_{ligand}$ (Figure 1l) mode. For $LESA_{ligand}$ mode, ligand binding was observed at concentrations of 10 μM and above (Figure S5, Supporting Information). There was no evidence for binding of multiple ligands at any concentration. No binding was observed for any of the ligands in the presence of 1% (v/v) formic acid (Figures S3−S5, Supporting Information).

The discrepancies in the concentrations at which the protein−ligand complexes were observed in the various sampling modes (direct infusion, $LESA_{premix}$, and $LESA_{ligand}$) together with the deviations in the observed relative abundance suggest that the extraction efficiency of LESA and the dilution inherent in the LESA sampling process result in changes to P_0 and/or L_0, thus shifting the equilibria described in eq 1. In order to calculate the K_d values from LESA data, it is necessary to determine the P_0 and L_0 values corrected for these factors.

https://doi.org/10.1021/jasms.2c00024
J. Am. Soc. Mass Spectrom. 2022, 33, 1168−1175

Table 1 shows the calculated K_d values obtained for CAH with the ligands CTZ, DNSA, and SLFA following direct infusion, $LESA_{premix}$, and $LESA_{ligand}$ MS together with those calculated from SPR measurements and literature values. (Examples of SPR sensograms for each ligand are given in Figure S6, Supporting Information, along with the derived binding parameters; see Table S1, Supporting Information.) The K_d values calculated for $LESA_{premix}$ and $LESA_{ligand}$ MS are given with (i) P_0 and L_0 corrected for the LESA extraction efficiency and dilution, (ii) only P_0 corrected for the LESA extraction efficiency and dilution, and (iii) uncorrected P_0 and L_0.

For CAH and CTZ, there is good agreement between the K_d values calculated from direct infusion MS, P_0- and L_0-corrected $LESA_{premix}$ MS, and SPR measurements. The measured values fall within the range described in the literature. For CAH and DNSA, there is good agreement between the K_d values measured by direct infusion and P_0- and L_0-corrected $LESA_{premix}$ MS. For CAH and SLFA, both the uncorrected and the corrected K_d values calculated from $LESA_{premix}$ MS are in reasonable agreement with those calculated by direct infusion MS. Differences between the reported K_d values from the SPR and MS measurements have been noted previously and the limitations discussed.[27] For the K_d values calculated from $LESA_{ligand}$ MS measurements, the best agreement with the K_d calculated from direct infusion MS for CTZ was achieved with the uncorrected value. For DNSA, neither corrected nor uncorrected $LESA_{ligand}$ values were in agreement with that obtained following direct infusion MS, although all were closer to those obtained by SPR. For SLFA, corrected values were in the best agreement with that obtained by direct infusion.

Calculation of K_d Values Following Direct Infusion and $LESA_{premix}$ MS. Conventionally, the K_d values are calculated from the direct infusion MS measurements after careful tuning, assuming that no major ligand dissociations occur in source or during detection and that the stoichiometry of a given protein−ligand (PL) complex formed in solution is maintained in the gas phase;[12] however, improved accuracy in the K_d values has been demonstrated when in-source dissociation is taken into account.[24,25] During LESA, the air-dried protein and/or protein−ligand spots are resolubilized and extracted from the substrate for MS. The extraction efficiency is below 100% if not all of the protein or ligand deposited is successfully extracted into the LESA droplet. Moreover, in the extraction process, the dried droplet is extracted into a larger volume (1.5 μL deposited sample volume extracted in 5 μL, i.e., ∼3.33-fold dilution). To address these factors, the extraction efficiencies of the protein and free ligand were determined, enabling us to calculate the corrected P_0 and L_0 values which were then used to determine the K_d values using eq 1.

First, we assumed that the extraction efficiencies of the free, unbound protein and the ligand-bound protein were the same. To account for the combined dilution and extraction efficiency effects for the protein, we deposited and extracted CAH mimicking the $LESA_{premix}$ conditions (Figure S7, Supporting Information) but collected the extracted sample rather than introducing it to the mass spectrometer. The protein concentration was determined by absorbance at 280 nm. An example of a representative absorption spectrum is shown in Figure S8, Supporting Information, for 10 μM CAH and 10 μM CAH following $LESA_{premix}$ sampling. The mean concentration (n = 15) after $LESA_{premix}$ sampling of 10 μM CAH protein spots was 1.51 ± 0.59 μM (Tables S2a and S2b, Supporting Information), indicating that the extraction efficiency was approximately 50%. These data also demonstrate the variation in protein sampling by LESA which can arise due to variable spreading of the sampling droplet, and therefore area sampled, and variation in the proportion of sampling solvent recovered on reaspiration.[52] The corrected protein concentration was used in subsequent K_d value calculations for the $LESA_{premix}$ conditions.

To estimate a correction factor for the combined effects of the $LESA_{premix}$-associated dilution and extraction efficiency for each ligand, we conducted LESA extraction, sample collection, and UV−vis spectrophotometry of the three compounds at various concentrations. A range of concentrations for each ligand without LESA sampling served as reference values. For all three ligands, the wavelength with maximum absorbance (λ_{max}) was determined experimentally (see Figure S9, Supporting Information, λ_{max} = 277 (CTZ), 244 (DNSA), and 258 nm (SLFA)) The absorbance at λ_{max} was plotted versus the ligand concentration, where it was evident that the mean absorbance values of the reference data points were higher than those following $LESA_{premix}$ sampling. A correction factor was calculated for each ligand across all points based on the ratio of the absorbance of the solution reference sample and the equivalent LESA sample. The mean correction factor was determined to be 0.32 ± 0.03 for CTZ, 0.33 ± 0.05 for DNSA, and 0.39 ± 0.08 for SLFA (Tables S3−S5, Supporting Information), indicating the extraction efficiencies were ∼100% for all concentrations after accounting for the dilution upon $LESA_{premix}$ sampling. These mean correction factors ± 1 STD were used to determine adjusted L_0 values for the $LESA_{premix}$ conditions.

The data used for K_d value determination by direct infusion and $LESA_{premix}$ are shown in Figure S10, Supporting Information. The results are summarized in Table 1. For CTZ and SLFA, the corrected and uncorrected K_d values do not differ significantly. For DNSA, however, the uncorrected K_d value is over 2-fold greater than that for direct infusion but correction of P_0 and L_0 results in good agreement between the K_d values determined by direct infusion MS and $LESA_{premix}$ MS.

Calculation of K_d Values Following $LESA_{ligand}$ MS. Our initial assumption for the $LESA_{ligand}$ mode was that only P_0 would require correction for LESA extraction efficiency and dilution, as the ligand is in the LESA solvent. We determined the corrected P_0 concentration by mimicking the $LESA_{ligand}$ sampling and collecting the sample for UV−vis spectrophotometry. A representative UV−vis spectrum is shown in Figure S11, Supporting Information. The mean extracted protein concentration (n = 10) was calculated to be 2.60 ± 0.62 μM (Table S6, Supporting Information). This value was used in subsequent K_d value calculations as the corrected P_0. Notably, this value is ∼2-fold higher than the value obtained for $LESA_{premix}$, likely due to the repeated mix steps in this LESA mode. (In addition, we could not rule out some solvent evaporation during the extended length of sampling, although the sample stage was kept covered at a constant 21 °C.) Individual titration plots used for determination of K_d values, with corrected P_0, can be found in Figure S12, Supporting Information.

The general lack of agreement between K_d values determined by direct infusion MS and $LESA_{ligand}$ MS despite

https://doi.org/10.1021/jasms.2c00024
J. Am. Soc. Mass Spectrom. 2022, 33, 1168−1175

correction of P_0 suggested that our assumption about L_0 was incorrect. We next considered whether the apparent L_0 after $LESA_{ligand}$ may increase as a consequence of evaporation during the 10 min sampling process. The sampling process, in which ligand solutions comprising a range of concentrations were deposited, aspirated, mixed, and reaspirated from the foil-covered slide, was recreated, and the resulting samples were collected. The absorbance spectra of these samples were compared with reference solutions that had not been subjected to any manipulation (Figure S13, Supporting Information). For DNSA and SLFA, the pairwise comparison of absorbances at the maximum wavelength (Figures S13f and S13i, Supporting Information) revealed that at higher concentrations L_0 was higher following $LESA_{ligand}$ sampling than that for the reference solution. Nevertheless, the mean correction factor across the concentration range was ∼1 in both cases (1.063 and 0.9904 for DNSA and SLFA, respectively, see Tables S7 and S8, Supporting Information). For CTZ, the pairwise comparison revealed higher absorbances for the $LESA_{ligand}$ samples at all concentrations (Figure S13c, Supporting Information). Moreover, a blue shift in the absorption spectrum was observed. The calculated mean correction factor was 1.5-fold higher than the initial ligand concentrations (Table S9, Supporting Information). The K_d values were calculated using corrected values for both P_0 and L_0 (see Table 1 and Figure S14, Supporting Information); however, the fits and agreement between values from direct infusion and $LESA_{premix}$ did not improve. For completeness, we also calculated the K_d values with no correction for P_0 and L_0 (Figure S14, Supporting Information). For CTZ, the uncorrected K_d value is in best agreement with the value obtained by direct infusion. For DNSA, correction of L_0 and/or P_0 did not significantly change the calculated K_d values. For SLFA, the corrected values were in better agreement than the uncorrected values. It is worth noting that the binding kinetics may also result in differences in the K_d values determined via $LESA_{premix}$ and $LESA_{ligand}$. For the protein−ligand interactions studied here, the calculated time to 99% occupancy was less than 10 min in all cases. For protein−ligand interactions with slower kinetics, it may be necessary to increase the incubation times ($LESA_{premix}$) or number of mix and repeat samples ($LESA_{ligand}$).

Structural Insights. We also considered whether the discrepancies seen for $LESA_{ligand}$ sampling might be due to conformational changes induced during the drying of the protein spots, that is, if structural changes and additional conformers are produced on drying which are maintained following LESA extraction then there is the possibility that a population of protein exists that is unable to bind ligand. To test that, we coupled native LESA MS with traveling wave ion mobility spectrometry for a single ligand concentration (30 μM) for each compound in the presence of controls. All mass spectra (Figure S15, Supporting Information) displayed a narrow charge state distribution from 8^+ to 11^+. The 8^+ ions showed multiple conformers (Figure S16, Supporting Information); however, the 8^+ charge state was not observed in high-resolution native MS and was not part of the titration plots described above. For the 9^+ charge state, two conformations were observed for CAH following LESA whereas a single peak was observed following direct infusion, as observed previously.[53] It is also possible that the 9^+ ion shows some heterogeneity in the gas phase, supported by the observation of two conformers with different CCSs reported by Harrison et al.[54] The drift time profiles for the ligand-bound CAH suggest binding to both the major and the minor conformers. The 10^+ and 11^+ ions were characterized by one main, dominant conformation in both direct infusion and LESA modes.

Table S10, Supporting Information, summarizes the estimated mean $^{TW}CCSs_{N2\rightarrow He}$ of the ligand-bound and free charge states and the CCSs of CAH only. Calculation of the $^{TW}CCSs_{N2\rightarrow He}$ in the presence of the three CAH inhibitors indicates that the coordination of these ligands in the active center of CAH do not result in a significant increase in $^{TW}CCSs_{N2\rightarrow He}$. Experimental CCS values yielded similar values for direct infusion, $LESA_{premix}$, and $LESA_{ligand}$ samples.

Finally, we assessed the near-UV secondary structure of CAH in the presence and absence of CTZ, DNSA, and SLFA in a range of concentrations. The circular dichroism spectra did not reveal any major conformational rearrangements in the secondary structure of the protein upon interactions with these ligands (Figure S17, Supporting Information).

CONCLUSIONS

The results show that native LESA MS is a potentially useful tool for quantitative determination of protein−ligand interactions using CAH and three inhibitors covering submicromolar to low micromolar K_d values as examples of monovalent interactions. To estimate the broader utility of LESA-MS, it would be particularly useful to examine a variety of larger proteins including those with a number of subunits capable of binding multiple ligands, proteins with multivalent binding sites, and proteins that bind numerous ligands with positive or negative cooperativity. When using LESA it is necessary to determine corrections for P_0 and L_0 to better describe the binding equilibrium following sampling from a substrate taking into account extraction efficiency and dilution effects. We found a good match between the K_d values derived from data obtained following direct infusion MS and $LESA_{premix}$ MS for all three ligands. In contrast, the K_d values from the $LESA_{ligand}$ sampling were inconsistent, and this could not be addressed by the corrections described here. We found that although $LESA_{ligand}$ MS is not suitable for accurate K_d value calculations, it can still confirm whether a ligand can bind or not, and CCS measurements can be observed with comparable values to those from direct infusion MS and $LESA_{premix}$ MS. Our findings suggest that native LESA MS has the potential to be developed as an automated, high-throughput platform to support drug development.

ASSOCIATED CONTENT

Supporting Information

The Supporting Information is available free of charge at https://pubs.acs.org/doi/10.1021/jasms.2c00024.

Extended methods, software for calculation of AUCs and fitting of titration curves, chemical structures of ligands, mass spectra, SPR sensograms and calculations, photographs of the advanced user interface, UV absorption spectra, calculation of corrected P_0 and L_0 values, titration plots, TWIMS mass spectra and drift time profiles, calculated collision cross sections, CD spectra (PDF)

Matlab AUC calculations; Python KD fitting (ZIP)

https://doi.org/10.1021/jasms.2c00024
J. Am. Soc. Mass Spectrom. 2022, 33, 1168−1175

AUTHOR INFORMATION

Corresponding Author

Helen J. Cooper − *School of Biosciences, University of Birmingham, Birmingham B15 2TT, United Kingdom;* orcid.org/0000-0003-4590-9384; Email: h.j.cooper@bham.ac.uk

Authors

Eva Illes-Toth − *School of Biosciences, University of Birmingham, Birmingham B15 2TT, United Kingdom*

Christopher J. Stubbs − *Mechanistic and Structural Biology, Discovery Sciences, R&D, AstraZeneca, Cambridge CB4 0WG, United Kingdom*

Emma K. Sisley − *School of Biosciences, University of Birmingham, Birmingham B15 2TT, United Kingdom*

Jeddidiah Bellamy-Carter − *School of Biosciences, University of Birmingham, Birmingham B15 2TT, United Kingdom;* orcid.org/0000-0002-1102-3596

Anna L. Simmonds − *School of Biosciences, University of Birmingham, Birmingham B15 2TT, United Kingdom*

Todd H. Mize − *School of Biosciences, University of Birmingham, Birmingham B15 2TT, United Kingdom*

Iain B. Styles − *School of Computer Science and Centre of Membrane Proteins and Receptors (COMPARE), University of Birmingham, Birmingham B15 2TT, United Kingdom; The Alan Turing Institute, London NW1 2DB, United Kingdom; University of Nottingham, Midlands NG7 2RD, United Kingdom;* orcid.org/0000-0002-6755-0299

Richard J. A. Goodwin − *Imaging and Data Analytics, Clinical Pharmacology & Safety Sciences, BioPharmaceuticals R&D, AstraZeneca, Cambridge CB4 0WG, United Kingdom*

Complete contact information is available at: https://pubs.acs.org/10.1021/jasms.2c00024

Notes

The authors declare no competing financial interest.

ACKNOWLEDGMENTS

E.I.T. and H.J.C. were funded by EPSRC (EP/R018367/1). H.J.C. is an EPSRC Established Career Fellow (EP/S002979). E.K.S. and A.L.S. received funding from the EPSRC via the Centre for Doctoral Training in Physical Sciences for Health (Sci-Phy-4-Health-EP/L016346/1). E.K.S.'s studentship was in collaboration with UCB Pharma. I.B.S. was supported by funding from the Alan Turing Institute. Supplementary data supporting this research is openly available from 10.25500/edata.bham.00000808.

REFERENCES

(1) Zinn, N.; Hopf, C.; Drewes, G.; Bantscheff, M. Mass spectrometry approaches to monitor protein-drug interactions. *Methods* **2012**, *57* (4), 430−440.

(2) Hansen, L. D.; Transtrum, M. K.; Quinn, C.; Demarse, N. Enzyme-catalyzed and binding reaction kinetics determined by titration calorimetry. *Biochim. Biophys. Acta* **2016**, *1860* (5), 957−966.

(3) Piliarik, M.; Vaisocherova, H.; Homola, J. Surface plasmon resonance biosensing. *Methods Mol. Biol.* **2009**, *503*, 65−88.

(4) Bacia, K.; Haustein, E.; Schwille, P. Fluorescence correlation spectroscopy: principles and applications. *Cold Spring Harb Protoc.* **2014**, *2014* (7), pdb.top081802.

(5) Goldflam, M.; Tarrago, T.; Gairi, M.; Giralt, E. NMR studies of protein-ligand interactions. *Methods Mol. Biol.* **2012**, *831*, 233−259.

(6) Nishida, N.; Shimada, I. An NMR method to study protein-protein interactions. *Methods Mol. Biol.* **2011**, *757*, 129−137.

(7) Eschweiler, J. D.; Kerr, R.; Rabuck-Gibbons, J.; Ruotolo, B. T. Sizing Up Protein-Ligand Complexes: The Rise of Structural Mass Spectrometry Approaches in the Pharmaceutical Sciences. *Annu. Rev. Anal Chem. (Palo Alto Calif)* **2017**, *10* (1), 25−44.

(8) Zhao, T.; King, F. L. Direct determination of the primary binding site of cisplatin on cytochrome C by mass spectrometry. *J. Am. Soc. Mass. Spectrom.* **2009**, *20* (6), 1141−1147.

(9) Cubrilovic, D.; Zenobi, R. Influence of dimehylsulfoxide on protein-ligand binding affinities. *Anal. Chem.* **2013**, *85* (5), 2724−2730.

(10) Woods, L. A.; Platt, G. W.; Hellewell, A. L.; Hewitt, E. W.; Homans, S. W.; Ashcroft, A. E.; Radford, S. E. Ligand binding to distinct states diverts aggregation of an amyloid-forming protein. *Nat. Chem. Biol.* **2011**, *7* (10), 730−739.

(11) Loo, J. A.; Hu, P.; McConnell, P.; Mueller, W. T.; Sawyer, T. K.; Thanabal, V. A study of Src SH2 domain protein—phosphopeptide binding interactions by electrospray ionization mass spectrometry. *J. Am. Soc. Mass Spectrom.* **1997**, *8* (3), 234−243.

(12) Kitova, E. N.; El-Hawiet, A.; Schnier, P. D.; Klassen, J. S. Reliable determinations of protein-ligand interactions by direct ESI-MS measurements. Are we there yet? *J. Am. Soc. Mass Spectrom.* **2012**, *23* (3), 431.

(13) Wang, Y.; Park, H.; Lin, H.; Kitova, E. N.; Klassen, J. S. Multipronged ESI-MS Approach for Studying Glycan-Binding Protein Interactions with Glycoproteins. *Anal. Chem.* **2019**, *91* (3), 2140−2147.

(14) El-Hawiet, A.; Kitova, E. N.; Arutyunov, D.; Simpson, D. J.; Szymanski, C. M.; Klassen, J. S. Quantifying ligand binding to large protein complexes using electrospray ionization mass spectrometry. *Anal. Chem.* **2012**, *84* (9), 3867.

(15) Vonderach, M.; Byrne, D. P.; Barran, P. E.; Eyers, P. A.; Eyers, C. E. DNA Binding and Phosphorylation Regulate the Core Structure of the NF-κB p50 Transcription Factor. *J. Am. Soc. Mass Spectrom.* **2019**, *30* (1), 128−138.

(16) Calabrese, A. N.; Bravo, J. P. K.; Cockburn, J. J. B.; Borodavka, A.; Tuma, R.; Barth, A.; Lamb, D. C.; Mojzes, P. Stability of local secondary structure determines selectivity of viral RNA chaperones. *Nucleic Acids Res.* **2018**, *46* (15), 7924−7937.

(17) Peschke, M.; Verkerk, U. H.; Kebarle, P. Features of the ESI mechanism that affect the observation of multiply charged non-covalent protein complexes and the determination of the association constant by the titration method. *J. Am. Soc. Mass. Spectrom.* **2004**, *15* (10), 1424−1434.

(18) Bovet, C.; Wortmann, A.; Eiler, S.; Granger, F.; Ruff, M.; Gerrits, B.; Moras, D.; Zenobi, R. Estrogen receptor-ligand complexes measured by chip-based nanoelectrospray mass spectrometry: an approach for the screening of endocrine disruptors. *Protein Sci.* **2007**, *16* (5), 938−46.

(19) Daniel, J. M.; Friess, S. D.; Rajagopalan, S.; Wendt, S.; Zenobi, R. Quantitative determination of noncovalent binding interactions using soft ionization mass spectrometry. *Internat. J. Mass Spectrom.* **2002**, *216* (1), 1−27.

(20) Cubrilovic, D.; Biela, A.; Sielaff, F.; Steinmetzer, T.; Klebe, G.; Zenobi, R. Quantifying protein-ligand binding constants using electrospray ionization mass spectrometry: a systematic binding affinity study of a series of hydrophobically modified trypsin inhibitors. *J. Am. Soc. Mass. Spectrom.* **2012**, *23* (10), 1768−77.

(21) Yao, Y.; Richards, M. R.; Kitova, E. N.; Klassen, J. S. Influence of Sulfolane on ESI-MS Measurements of Protein-Ligand Affinities. *J. Am. Soc. Mass. Spectrom.* **2016**, *27* (3), 498−506.

(22) Sobott, F.; McCammon, M. G.; Hernandez, H.; Robinson, C. V. The flight of macromolecular complexes in a mass spectrometer. *Phil. Trans. R. Soc. A.* **2005**, *363* (1827), 379−391.

(23) Gabelica, V.; Vreuls, C.; Filée, P.; Duval, V.; Joris, B.; Pauw, E. D. Advantages and drawbacks of nanospray for studying noncovalent protein-DNA complexes by mass spectrometry. *Rapid Commun. Mass Spectrom.* **2002**, *16* (18), 1723−8.

(24) Báez Bolivar, E. G.; Bui, D. T.; Kitova, E. N.; Han, L.; Zheng, R. B.; Luber, E. J.; Sayed, S. Y.; Mahal, L. K.; Klassen, J. S. Submicron

Emitters Enable Reliable Quantification of Weak Protein-Glycan Interactions by ESI-MS. *Anal. Chem.* **2021**, *93* (9), 4231−4239.
(25) Jaquillard, L.; Saab, F.; Schoentgen, F.; Cadene, M. Improved Accuracy of Low Affinity Protein-Ligand Equilibrium Dissociation Constants Directly Determined by Electrospray Ionization Mass Spectrometry. *J. Am. Soc. Mass Spectrom.* **2012**, *23* (5), 908−922.
(26) Zhang, S.; Van Pelt, C. K.; Wilson, D. B. Quantitative determination of noncovalent binding interactions using automated nanoelectrospray mass spectrometry. *Anal. Chem.* **2003**, *75* (13), 3010.
(27) Jecklin, M. C.; Schauer, S.; Dumelin, C. E.; Zenobi, R. Label-free determination of protein-ligand binding constants using mass spectrometry and validation using surface plasmon resonance and isothermal titration calorimetry. *Journal of molecular recognition: JMR* **2009**, *22* (4), 319−329.
(28) Kertesz, V.; Van Berkel, G. J. Fully automated liquid extraction-based surface sampling and ionization using a chip-based robotic nanoelectrospray platform. *J. Mass Spectrom.* **2010**, *45* (3), 252−260.
(29) Griffiths, R. L.; Sisley, E. K.; Lopez-Clavijo, A. F.; Simmonds, A. L.; Styles, I. B.; Cooper, H. J. Native mass spectrometry imaging of intact proteins and protein complexes in thin tissue sections. *Int. J. Mass Spectrom.* **2019**, *437*, 23−29.
(30) Hale, O. J.; Cooper, H. J. Native Mass Spectrometry Imaging and In Situ Top-Down Identification of Intact Proteins Directly from Tissue. *J. Am. Soc. Mass Spectrom.* **2020**, *31* (12), 2531−2537.
(31) Sisley, E. K.; Hale, O. J.; Styles, I. B.; Cooper, H. J. Native ambient mass spectrometry imaging of ligand-bound and metal-bound proteins in rat brain. *J. Am. Chem. Soc.* **2022**, *144*, 2120−2128.
(32) Burbaum, J. J.; Ohlmeyer, M. H.; Reader, J. C.; Henderson, I.; Dillard, L. W.; Li, G.; Randle, T. L.; Sigal, N. H.; Chelsky, D.; Baldwin, J. J. A paradigm for drug discovery employing encoded combinatorial libraries. *Proc. Natl. Acad. Sci. U. S. A.* **1995**, *92* (13), 6027−6031.
(33) Day, Y. S.; Baird, C. L.; Rich, R. L.; Myszka, D. G. Direct comparison of binding equilibrium, thermodynamic, and rate constants determined by surface- and solution-based biophysical methods. *Protein Sci.* **2002**, *11* (5), 1017−1025.
(34) Winum, J.-Y.; Cecchi, A.; Montero, J.-L.; Innocenti, A.; Scozzafava, A.; Supuran, C. T. Carbonic anhydrase inhibitors. Synthesis and inhibition of cytosolic/tumor-associated carbonic anhydrase isozymes I, II, and IX with boron-containing sulfonamides, sulfamides, and sulfamates: Toward agents for boron neutron capture therapy of hypoxic tumors. *Bioorg. Med. Chem. Lett.* **2005**, *15* (13), 3302−3306.
(35) Conroy, C. W.; Maren, T. H. The effect of temperature on the binding of sulfonamides to carbonic anhydrase isoenzymes I, II, and IV. *Mol. Pharmacol.* **1995**, *48* (3), 486−491.
(36) Supuran, C. T. How many carbonic anhydrase inhibition mechanisms exist? *J. Enzyme Inhib. Med. Chem.* **2016**, *31* (3), 345−360.
(37) Lindskog, S.; Coleman, J. E. The catalytic mechanism of carbonic anhydrase. *Proc. Natl. Acad. Sci. U. S. A.* **1973**, *70* (9), 2505−2508.
(38) McKenna, R.; Supuran, C. T. Carbonic anhydrase inhibitors drug design. *Subcell. Biochem.* **2014**, *75*, 291−323.
(39) Saito, R.; Sato, T.; Ikai, A.; Tanaka, N. Structure of bovine carbonic anhydrase II at 1.95 A resolution. *Acta Crystallogr. D Biol. Crystallogr.* **2004**, *60* (4), 792−795.
(40) Winum, J. Y.; Cecchi, A.; Seridi, A.; Scozzafava, A.; Montero, J. L.; Supuran, C. T. Carbonic anhydrase inhibitors. N-cyanomethyl-sulfonamides-a new zinc binding group in the design of inhibitors targeting cytosolic and membrane-anchored isoforms. *J. Enzyme Inhib. Med. Chem.* **2006**, *21* (4), 477−381.
(41) Krishnamurthy, V. M.; Kaufman, G. K.; Urbach, A. R.; Gitlin, I.; Gudiksen, K. L.; Weibel, D. B.; Whitesides, G. M. Carbonic Anhydrase as a Model for Biophysical and Physical-Organic Studies of Proteins and Protein-Ligand Binding. *Chem. Rev.* **2008**, *108* (3), 946−1051.
(42) Krishnamurthy, V. M.; Bohall, B. R.; Semetey, V.; Whitesides, G. M. The Paradoxical Thermodynamic Basis for the Interaction of Ethylene Glycol, Glycine, and Sarcosine Chains with Bovine Carbonic Anhydrase II: An Unexpected Manifestation of Enthalpy/Entropy Compensation. *J. Am. Chem. Soc.* **2006**, *128* (17), 5802−5812.
(43) King, R. W.; Burgen, A. S. Kinetic aspects of structure-activity relations: the binding of sulphonamides by carbonic anhydrase. *Proc. R. Soc. London, Ser. B* **1976**, *193* (1111), 107−125.
(44) Nair, S. K.; Elbaum, D.; Christianson, D. W. Unexpected binding mode of the sulfonamide fluorophore 5-dimethylamino-1-naphthalene sulfonamide to human carbonic anhydrase II. Implications for the development of a zinc biosensor. *J. Biol. Chem.* **1996**, *271* (2), 1003−1007.
(45) Myszka, D. G. Kinetic analysis of macromolecular interactions using surface plasmon resonance biosensors. *Curr. Opin. Biotechnol.* **1997**, *8* (1), 50−57.
(46) Myszka, D. G.; Abdiche, Y. N.; Arisaka, F.; Byron, O.; Eisenstein, E.; Hensley, P.; Thomson, J. A.; Lombardo, C. R.; Schwarz, F.; Stafford, W.; Doyle, M. L. The ABRF-MIRG'02 study: assembly state, thermodynamic, and kinetic analysis of an enzyme/inhibitor interaction. *J. Biomol. Tech.* **2003**, *14* (4), 247−269.
(47) Bootorabi, F.; Jänis, J.; Valjakka, J.; Isoniemi, S.; Vainiotalo, P.; Vullo, D.; Supuran, C. T.; Waheed, A.; Sly, W. S.; Niemelä, O.; Parkkila, S. Modification of carbonic anhydrase II with acetaldehyde, the first metabolite of ethanol, leads to decreased enzyme activity. *BMC Biochem.* **2008**, *9* (1), 32.
(48) Zhuang, X.; Gavriilidou, A. F. M.; Zenobi, R. Influence of Alkylammonium Acetate Buffers on Protein-Ligand Noncovalent Interactions Using Native Mass Spectrometry. *J. Am. Soc. Mass. Spectrom.* **2017**, *28* (2), 341−346.
(49) Banerjee, A. L.; Tobwala, S.; Ganguly, B.; Mallik, S.; Srivastava, D. K. Molecular basis for the origin of differential spectral and binding profiles of dansylamide with human carbonic anhydrase I and II. *Biochem.* **2005**, *44* (10), 3673−3682.
(50) Morcos, E. F.; Kussrow, A.; Enders, C.; Bornhop, D. Free-solution interaction assay of carbonic anhydrase to its inhibitors using back-scattering interferometry. *Electrophoresis* **2010**, *31* (22), 3691−3695.
(51) Cannon, M. J.; Papalia, G. A.; Navratilova, I.; Fisher, R. J.; Roberts, L. R.; Worthy, K. M.; Stephen, A. G.; Marchesini, G. R.; Collins, E. J.; Casper, D.; Qiu, H.; Satpaev, D.; Liparoto, S. F.; Rice, D. A.; Gorshkova, I. I.; Darling, R. J.; Bennett, D. B.; Sekar, M.; Hommema, E.; Liang, A. M.; Day, E. S.; Inman, J.; Karlicek, S. M.; Ullrich, S. J.; Hodges, D.; Chu, T.; Sullivan, E.; Simpson, J.; Rafique, A.; Luginbühl, B.; Westin, S. N.; Bynum, M.; Cachia, P.; Li, Y.-J.; Kao, D.; Neurauter, A.; Wong, M.; Swanson, M.; Myszka, D. G. Comparative analyses of a small molecule/enzyme interaction by multiple users of Biacore technology. *Anal. Biochem.* **2004**, *330* (1), 98−113.
(52) Havlikova, J.; Randall, E. C.; Griffiths, R. L.; Swales, J. G.; Goodwin, R. J. A.; Bunch, J.; Styles, I. B.; Cooper, H. J. Quantituve imaging pf proteins in tissue by stable isotope labeled mimetic liquid extraction surface analysis mass spectrometry. *Anal. Chem.* **2019**, *91*, 14198−14202.
(53) Illes-Toth, E.; Cooper, H. J. Probing the Fundamentals of Native Liquid Extraction Surface Analysis Mass Spectrometry of Proteins: Can Proteins Refold during Extraction? *Anal. Chem.* **2019**, *91* (19), 12246−12254.
(54) Harrison, J. A.; Kelso, C.; Pukala, T. L.; Beck, J. L. Conditions for Analysis of Native Protein Structures Using Uniform Field Drift Tube Ion Mobility Mass Spectrometry and Characterization of Stable Calibrants for TWIM-MS. *J. Am. Soc. Mass. Spectrom.* **2019**, *30* (2), 256−267.

https://doi.org/10.1021/jasms.2c00024
J. Am. Soc. Mass Spectrom. 2022, 33, 1168−1175